PERGAMON

European Journal of Cancer 36 (2000) 2368–2374

European Journal of Cancer

www.ejconline.com

The homeobox gene *MEIS1* is amplified in IMR-32 and highly expressed in other neuroblastoma cell lines

T.A. Jones [a,†], R.H. Flomen [b,†], G. Senger [c], D. Nižetić [b], D. Sheer [a,*]

[a] *Human Cytogenetics Laboratory, Imperial Cancer Research Fund, P.O. Box 123, Lincoln's Inn Fields, London WC2A 3PX, UK*
[b] *Centre for Applied Molecular Biology, School of Pharmacy, University of London, 29/39 Brunswick Square, London WC1N 1AX, UK*
[c] *Practice of Medical Genetics and Gynaecology, Roritzerstr. 2, 93049 Regensburg, Germany*

Received 13 April 2000; received in revised form 24 July 2000; accepted 16 August 2000

Abstract

Neuroblastoma is a childhood tumour of the sympathetic nervous system that demonstrates striking clinical heterogeneity. In order to determine which genes are abnormally expressed in neuroblastoma, we screened regions of amplification from the short arm of chromosome 2 in the neuroblastoma cell line IMR-32 and found that the homeobox gene, myeloid ecotropic integration site 1 (*MEIS1*), is highly amplified. *MEIS1* normally maps to chromosome band 2p14. High expression of *MEIS1* without amplification was also found in other neuroblastoma cell lines, with and without *MYCN* amplification, and in medulloblastoma and erythroleukaemia cell lines. *MEIS1* is highly expressed in cerebellum and ubiquitously expressed in normal immunohaematopoietic tissues and is thought to be important in cell proliferation and differentiation. While several lines of evidence point towards a role for homeobox genes in the development of other malignancies, this is the first report showing the amplification of a homeobox gene in neuroblastoma.

Keywords: *MEIS1*; Neuroblastoma; IMR-32; Amplification; Expression

1. Introduction

Neuroblastoma is one of the commonest solid tumours in young children, constituting 10% of all cancers in children under 15 years of age. It arises as an embryonal tumour of the sympathetic nervous system, but demonstrates clinical heterogeneity, with the clinical course ranging from spontaneous regression to extremely aggressive tumour behaviour. Low, intermediate and high-risk groups of patients are associated with distinct molecular genetic and biological features [1]. Favourable features include early stage (1, 2A, 2B or 4S), age at diagnosis less than 1 year, triploid karyotype, lack of 1p abnormalities and the absence of *MYCN* amplification. Unfavourable features are advanced stage (3 or 4), age over 1 year, pseudodiploid and tetraploid karyotypes, deletion of the short arm of chromosome 1, *MYCN* amplification and gain of the long arm of chromosome 17 [2]. Patients with these features frequently have poor prognosis, showing little response even to aggressive multi-agent chemotherapy.

The relative contributions to tumorigenesis of *MYCN* amplification and other genes affected by chromosome aberrations in neuroblastoma are currently unknown. Several genes may be co-amplified with *MYCN* in neuroblastoma, yet none are amplified in the absence of *MYCN* amplification. One of these, the DEAD box motif gene *DDX1*, is amplified in 60–70% of *MYCN*-amplified neuroblastomas [3]. *DDX1* has been mapped to a position 340 kb 5′ and telomeric to *MYCN* in chromosome band 2p24 [4]. More recently, neuroblastoma amplified gene (*NAG*) was also shown to be co-amplified in 70% of *MYCN*-amplified neuroblastomas and to map telomeric to *MYCN* [5]. The gene ornithine decarboxylase (*ODC1*) in chromosome band 2p25, is occasionally co-amplified with *MYCN* and is thought to be at the border of the region of DNA which is usually co-amplified [6]. Since a correlation between *MYCN* and *ODC1* expression has been noted in neuroblastoma cell lines, it has been suggested that

* Corresponding author. Tel.: +44 20 7269 3220; fax: +44 20 7269 3655.
E-mail address: d.sheer@icrf.icnet.uk (D. Sheer).
† Joint first authors.

0959-8049/00/$ - see front matter
PII: S0959-8049(00)00332-4

MYCN may be the natural regulator of *ODC1* expression in neuronal tumours [7].

In this study, we investigated the genomic regions which are co-amplified with *MYCN* in the neuroblastoma cell line IMR-32. The cell line was established from an abdominal mass in a 13-month-old Caucasian male [8], and contains two copies of a large sub-metacentric chromosome, der(1), resulting from a non-reciprocal translocation between chromosomes 1 and 17. This large marker chromosome contains a homogeneously staining region (HSR) carrying amplified *MYCN*, flanked by material from chromosome 17 [9].

We show here that the homeobox gene *MEIS1* is present in multiple copies in this HSR in IMR-32, where it is highly expressed. The gene is also highly expressed in other neuroblastoma and medulloblastoma cell lines where it is not amplified. We discuss these findings in the context of homeobox genes in neural development and tumorigenesis.

2. Materials and methods

2.1. Cell culture and chromosome preparation

The following cell lines were obtained from the American Type Culture Collection (ATCC, Manassas, USA) and cultured using recommended conditions: neuroblastoma cell lines IMR-32 (from an abdominal mass), SK-N-AS, SK-N-Be, SK-N-DZ, SK-N-FI (all from bone marrow metastases), CHP212, Kelly (both from brain), and SK-N-LI; medulloblastoma cell lines HTB186 (desmoplastic cerebellar medulloblastoma), D283 (metastatic medulloblastoma) and TE671 (subline No. 2); erythroleukaemia cell line HEL 92.1.7 (megakaryocytic-erythroid); and the chronic myeloid leukaemia cell line K-562 (megakaryocytic-erythroid). In addition, the follicular thyroid carcinoma cell line RO82-W-1 was obtained from the European Collection of Cell Cultures. In order to obtain metaphase chromosomes, cells were treated with colcemid (0.04 μg/ml) for 45 min, followed by a hypotonic treatment in 0.4% potassium chloride for 25 min at 37°C and fixation in 3:1 methanol–glacial acetic acid. Slides were air-dried and stored desiccated at −20°C until required.

2.2. Libraries used

CEPH mega-YAC (yeast artificial chromosome) library high-density filters [10], human genomic P1 clone (PAC) library RPCI-1 high-density filters [11] and individual clones from the I.M.A.G.E consortium (http://bbrp.llnl.gov/bbrp/image) [12] were all kindly provided by the UK HGMP Resource Centre, Hinxton.

2.3. Probes

Probes used were *MYCN* (pNb-1) (kindly provided by J. Lunec), *DDX1* 13.5 kb genomic clone, lambda 2001, spanning from exon 4 to 10 of the *DDX1* gene (kindly provided by J. Squire), myeloid ecotropic viral integration site 1 (*MEIS1*) I.M.A.G.E. clone 223490 (provided by the Medical Research Council (MRC) HGMP Resource Centre, UK) and *β-actin*. The HSR on the der(1) chromosome was microdissected, amplified and labelled either with biotin-16-dUTP (BRL) or with α-[^{32}P] dCTP (ICN) by degenerate oligonucleotide polymerase chain reaction (DOP-PCR). *V-REL* avian reticuloendotheliosis virus oncogene 1 kb genomic clone pKW101 mapped to 2p13 (ATCC). Cell determinant *(CD)8A* 1.1 kb cDNA mapped to 2p12 and transforming growth factor *(TGF)A* two clones of 3.4 kb and 925 bp, respectively, mapped to 2p13 (all from the HGMP resource centre). Follicle stimulating hormone (*FSH*) receptor 1.64 kb cDNA mapped to 2p16-p21 (kindly provided by T. Minegishi, Gunma University, Japan). *hMSH2* P1 clones M1015 and M1016 mapped to 2p16 (kindly provided by N. Papadopoulos, The Johns Hopkins Oncology Center, Baltimore, MD, USA). Glutamine: fructose 6-phosphate amidotransferase (*GFAT*) lambda clones 1a and 15aX1 mapped to 2p13 (kindly provided by T.E. Whitmore, Zymogenetics, Washington, DC, USA) and early growth response (EGR)4 4.5 kb genomic clone pAT133 mapped to 2p13 (kindly provided by P. F. Zipfel, Bernhard Nocht Institute, Hamburg, Germany). PCR probes specific to the 5′ and 3′ untranslated regions (UTRs) of *MEIS1* were generated using the following primers:

*MEIS*5′F ACACTGGCCTTAAAGAGG 3′, *MEIS*5′R TGCCTACTCCATCCATGC (450 bp)

*MEIS*3′F TCCATAGCTCTTCACTTCC, *MEIS*3′R GCTTGATGTGACAATTAGG (370 bp)

2.4. Commercial Poly A^+ mRNA

Commercial Poly A^+ mRNA was obtained for human brain, cerebellum, human bone marrow, human pancreas, human fetal liver, human fetal brain, human lung carcinoma (A549), human chronic myeloid leukaemia (K-562) and human Burkitt's lymphoma (Daudi) all from Clontech Laboratories Inc., Palo Alto, CA, USA.

2.5. *Fluorescence* in situ *hybridisation (FISH)*

Standard FISH techniques were used [13]. Briefly, 200 ng probe DNA was mixed with 5 μg Cot-1 DNA (Life Technologies, Paisley, UK), precipitated, denatured, allowed to pre-anneal, and then applied to a denatured slide and hybridised at 37°C overnight. Slides were washed and biotin/digoxigenin visualised with avidin–fluorescein

isothiocyanate (FITC)/anti-digoxigenin-rhodamine, yielding green and red signals, respectively. Slides were counterstained with DAPI (4, 6-diamidino-2-phenylindole) and then mounted in Citifluor. Images were captured using a Zeiss Axioskop epifluorescence microscope equipped with a Photometrics KAF 14500-500 CCD camera connected to an Apple PowerMac 8100 computer. Separate images of probe signal and DAPI counterstain were pseudocoloured and merged using SmartCapture software (Vysis, Inc., Chicago, IL, USA).

2.6. Comparative genomic hybridisation (CGH)

CGH analysis of primary neuroblastoma tumours and cell lines was performed using standard techniques [14]. Briefly, genomic tumour DNA and reference DNA were directly labelled with fluorescein-12-dCTP (Dupont NEN, Zaventem, Belgium) and Texas Red-5-dCTP (Dupont NEN), respectively. Equal amounts (300 ng) of tumour and reference DNA were mixed and precipitated with 30 μg Cot-1 DNA (Life Technologies). DNA samples were dissolved in hybridisation mixture (50% formamide/2×SSC at pH 7.0) and denatured for 5 min at 85°C. The probe mixture was allowed to preanneal, applied to a denatured slide and hybridised for 48 h. Slides were then washed and counterstained with DAPI in Citifluor. Slides were analysed using SmartCapture software (Vysis).

2.7. PAC library screen, gridding and DNA preparation of positive clones

The RPCI-1 Human PAC library was screened with HSR DNA which was labelled with α-[^{32}P] dCTP using DOP PCR [15]. Positive clones were picked into 384 plates containing 2×YT and 30 μg/ml kanamycin. Following overnight incubation at 37°C, glycerol was added to a final concentration of 20% (v/v). Gridding and growing clones on Hybond N+ and subsequent filter processing was carried out as described by Bentley and colleagues [16]. For DNA isolation, positive clones were grown for 14 h in 15 ml of super-broth (32 g tryptone, 20 g yeast extract, 5 g NaCl, 5 ml 1 N NaOH per litre) with 30 μg/ml kanamycin. DNA was isolated using a modified alkaline lysis method [17].

2.8. PAC insert preparation and restriction analysis

0.5–1 mg of PAC DNA was digested at 37°C with one or a combination of the following restriction enzymes: *Not*I, *Sal*I (NEB), *Xho*I or *Eco*RI (Life Technologies). Pulsed field gel electrophoresis (PFGE) was carried out using a CHEF-DR II system (BIO-RAD Laboratories Ltd, Hemel Hempstead, UK) according to the manufacturer's recommendations. Running conditions were as follows: 5.2 V/cm, 14 h, switch time 3–15 s. PAC inserts were prepared by digesting the PAC DNA with *Not*I. The insert fragment was cut from the pulsed field gel (PFG) and prepared as described by Groet and colleagues [18]. For rare cutter mapping of fragments less than 3 kb and for *Eco*RI fingerprinting of appropriate PACs, digestion reactions were analysed on standard 0.8% agarose gels.

2.9. Reverse transcriptase-polymerase chain reaction (RT–PCR)

mRNA was prepared from all cell lines using the MicroFast Track kit (Invitrogen). Commercial PolyA$^+$ mRNA was obtained from Clontech for human cerebellum, human bone marrow, brain, K-562 (human chronic myeloid leukaemia cell line), Daudi (human Burkitt's lymphoma cell line) and A549 (human lung carcinoma cell line). The Dipstick kit (Invitrogen) was used to determine the concentration of mRNA before cDNA synthesis using the First-Strand cDNA synthesis kit from Amersham Pharmacia Biotech (Bucks, UK). RT–PCR was carried out using 100–300 ng of mRNA and 2.5 units of Taq in a final volume of 50 μl using a Peltier Thermal Cycler (MJ Research, MA, USA). Primers were designed as 18 mers which gave a 400 bp product, *ME1S*3′R: 5′-GCT TGA TGT GAC AAT TAG-3′ and *ME1S*3′F: 5′-TCC ATA GCT CTT CAC TTC-3′. Cycling conditions were as follows: an initial incubation at 95°C for 5 min, followed by 35 cycles of denaturation (93°C, 1 min), annealing (58°C, 1 min) and extension (72°C, 3 min). A final step of 72°C for 5 min was added.

2.10. Northern blot analysis

Approximately 2 μg mRNA was loaded into each lane of a denaturing formaldehyde gel [17] and electrophoresed for 5 h at 55 V before northern transfer to a Hybond N$^+$ membrane. *MEIS1* and *MYCN* probes were radiolabelled with α-[^{32}P] dCTP (specific activity, 1–2×10^6-cpm/ml hybridisation mixture) and hybridisation performed using ExpressHyb hybridisation solution (Clontech). Washing was performed to a final stringency of 0.1×standard saline citrate (SSC) and 0.1% sodium dodecyl sulphate (SDS) at 50°C. The filters were then exposed to Molecular Dynamics Phosphorimager screens. Quantitation of loading was confirmed by stripping the filter and rehybridising to a probe for *β-actin*.

3. Results

3.1. CGH and FISH analysis

Genomic regions 2p24-p23, 2p16 and 2p14 were found by CGH to be amplified in IMR-32 cells (data

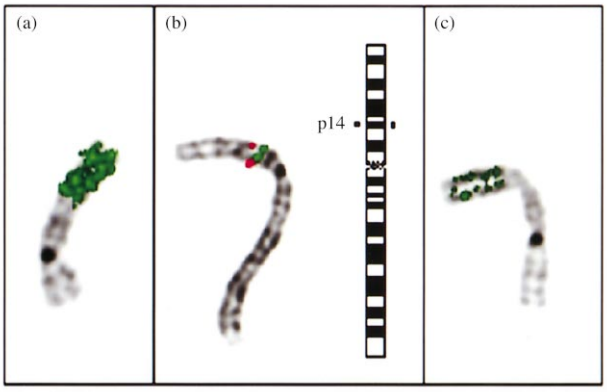

Fig. 1. Amplification of: (a) *MYCN* (pNb-1); and (c) myeloid ecotropic integration site 1 (*MEIS1*) (I.M.A.G.E. clone 223490) along the p arm of the derivative chromosome 1 in the cell line IMR-32. Biotinylated probes were detected with avidin–fluoresceinisothiocyanate (FITC). Fluorescence *in situ* hybridisation (FISH) of *DDX1* (lambda 2001) onto IMR-32 also showed amplification (data not shown). (b) Two-colour FISH to normal human chromosome 2 showing the order: telomere — group II (PAC 172B3) (Texas Red) — group I (PAC 2E20) (FITC) — centromere.

not shown). The HSR contained within the derivative chromosome 1 was then microdissected, and shown by FISH to be derived from bands 2p24, 2p23, 2p16 and 2p14, confirming the CGH results. An initial screen by FISH using probes available for genes mapping to our regions of interest along chromosome arm 2p showed the following genes were not present in the HSR: *VREL*, *CD8A*, *TGFA*, *FSH*, *hMSH2*, *GFAT* and *EGR4* (data not shown). FISH using *MYCN* and *DDX1*, both of which map to 2p24, showed clear amplification of both genes in the HSR (Fig. 1a for *MYCN* amplification).

3.2. Library screen

DNA from the microdissected HSR was then used to screen the RPCI-1 Human PAC library for probes representing the amplified sequences. 52 PACs were isolated and mapped as follows: 34 PACs on band 2p24, 3 PACs on band 2p23, 1 PAC on band 2p16 and 14 PACs on band 2p14. All the PACs were then shown by FISH to be amplified in the HSR of IMR-32.

3.3. Contig construction and restriction mapping of PACs at 2p14

We considered that co-amplification of a genomic region several Mb away from *MYCN* is unlikely to have no phenotypic effect and may provide a growth advantage to the cell. We, therefore, analysed PACs located on band 2p14, which constituted the majority of PACs not localised to band 2p24. PACs were grouped in the first instance by *Eco*RI fingerprinting and hybridisation of entire PAC inserts to gridded filters of the relevant clones. The two major PAC contigs assembled in this way (groups I and II, see Fig. 2) were then restriction mapped using the rare cutting enzymes *Not*I, *Sal*I and *Xho*I. Overlaps between clones and their T7/SP6

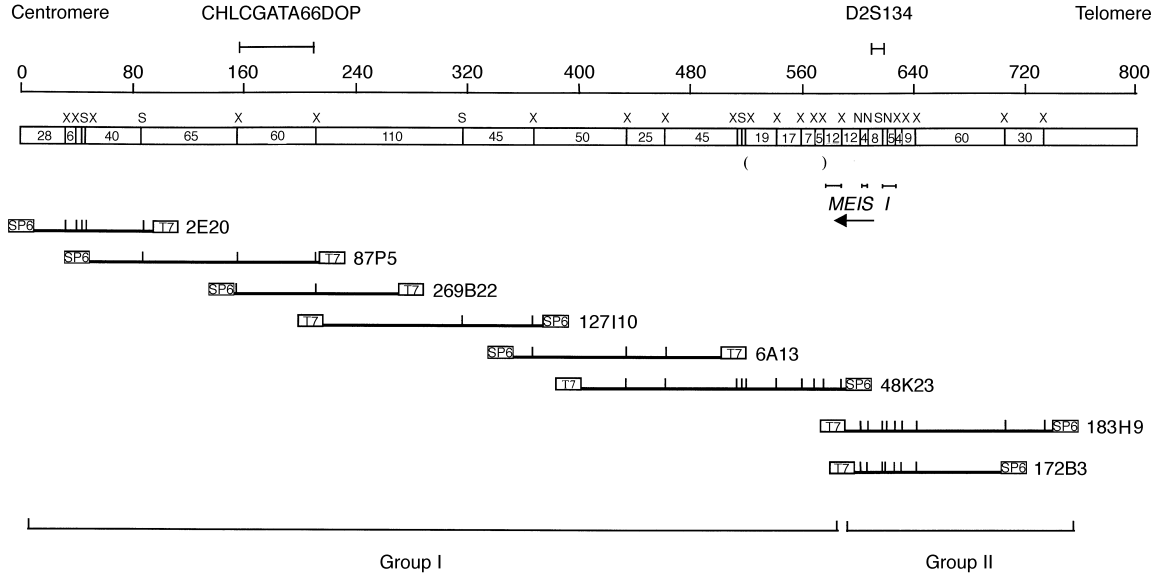

Fig. 2. PAC contig. The scale in kb is shown at the top of the figure, with the positions of sequence tagged site (STS) markers and centromere/telomere orientation indicated above. The open bar below is a representation of genomic DNA showing the positions of *Xho*I (X), *Sal*I (S) and *Not*I (N) restriction enzyme sites. Sizes of restriction fragments are shown by vertical lines within the open bar. The location of the *MEIS1* gene is indicated directly below the open bar and genomic fragments containing gene coding sequences are marked with horizontal bars. The arrow indicates the 5′ to 3′ orientation of the gene. Brackets beneath the open bar show that the order of these *Xho*I sites has not been determined. The lower part of the figure comprises the PAC contig, with SP6/T7 vector ends boxed and restriction enzyme sites denoted by vertical lines attached to the PACs. The positions of the original two groups of clones are marked beneath the PAC contig.

orientation were confirmed by hybridisation of PAC end fragments to Southern blots of the appropriate restriction digested clones. The two separate contigs were ordered with respect to the chromosome by hybridising one PAC from each group to prometaphase chromosomes. 124/155 cells (80%) showed the order: telomere–group II–group I–centromere (Fig. 1b). Contigs I and II were then linked by hybridisation of the SP6 vectorette PCR end [18] of PAC 48K23 to PACs 183H9 and 172B3 (Fig. 2).

3.4. *Identification and characterisation of* MEIS1

The CEPH mega-YAC library was screened with selected PAC inserts. A series of overlapping YACs in the region was identified using the Whitehead Institute website (*http://www.genome.wi.mit.edu/*), and Genethon markers at 2p14 confirmed by direct PCR of YAC colonies. Unigenes mapping to radiation hybrids containing these markers (*http://www.ncbi.nlm.nih.gov/genemap99*) were obtained as I.M.A.G.E. clones (*http://bbrp.llnl.gov/bbrp/image*) and hybridised to the YAC and PAC contigs. The homeobox gene, *MEIS1*, was mapped onto the PAC contig using a 2.5 kb I.M.A.G.E. clone (223490) that represents the majority of the 3.5 kb *MEIS1* transcript [19]. Additional information was obtained using PCR from the 5′ and 3′ (UTRs) of *MEIS1* (*MEIS*5′F/R and *MEIS*3′F/R respectively). As shown in Fig. 2, *MEIS1* is located towards the telomeric end of the 2p14 PAC contig at the CpG island within PACs 183H9 and 172B3. The gene is transcribed in a telomere–centromere orientation and clone 223490 hybridises to the three genomic fragments indicated within PACs 183H9/172B3 and 48K23. These mapping data indicate that the *MEIS1* gene spans at least 43 kb of genomic DNA. PCR using primers specific to the 5′ and 3′ UTRs confirmed that these mapped within PACs 183H9/172B3 and 48K23, respectively.

FISH using the 2.5 kb *MEIS1* I.M.A.G.E. clone 223490 on metaphase spreads from IMR-32 showed amplification along the HSR (Fig. 1c). *MYCN* has previously been shown to be amplified in the neuroblastoma cell lines IMR-32 (30-fold), Kelly (120-fold), SK-N-Be (150-fold), SK-N-DZ, and CHP212, but not in the cell lines SK-N-AS, SK-N-LI and SK-N-FI. However, amplification of *MEIS1* was not found in any other neuroblastoma, medulloblastoma or erythroleukaemia cell line analysed in this study.

3.5. *Expression of* MEIS1 *in IMR-32*

RT-PCR using primers (*ME1S*3′R and *ME1S*3′F) showed expression of *MEIS1* in all cell lines analysed except for the Burkitt's lymphoma cell line, Daudi (Fig. 3). The controls lacking reverse transcriptase were negative for all samples (data not shown). Northern blot analysis was performed on selected cell lines to determine whether amplification of *MEIS1* correlated with expression levels. Strong expression of *MEIS1* was found in the neuroblastoma cell lines IMR-32, SK-N-AS, SK-N-DZ and CHP212. A lower level of expression was observed in the cell line SK-N-Be (Fig. 4). The 5 kb and 3.5 kb transcripts were also observed in the medulloblastoma cell lines HTB186 and TE671 and in the erythroleukaemia line HEL 92.1.7 (data not shown). After correcting for differences in loading (see actin control bands), similar expression of *MEIS1* was observed in all neuroblastoma cell lines. However, in relation to IMR-32, *MEIS1* expression was 5-fold higher in SK-N-AS and 2- to 3-fold lower in SK-N-Be. Although expression levels of *MYCN* in these cell lines correlates with copy number, expression of *MEIS1* is much higher in

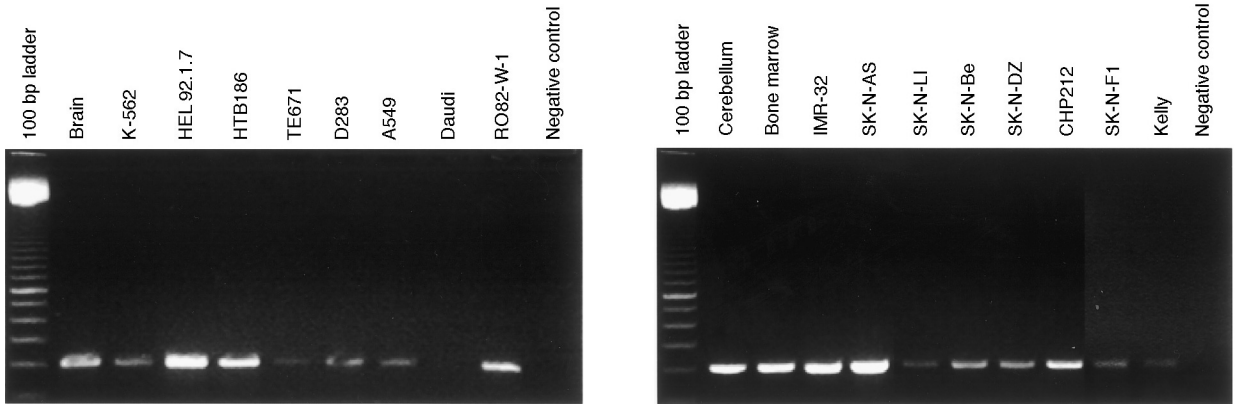

Fig. 3. Reverse transcriptase-polymerase chain reaction (RT-PCR) showing myeloid ecotropic integration site 1 (*MEIS1*) expression. Ubiquitous expression is shown in normal cerebellum, bone marrow and brain, the neuroblastoma cell lines (IMR-32, SK-N-AS, SK-N-FI, Kelly, SK-N-LI, SK-N-Be, SK-N-DZ and CHP212), the medulloblastoma cell lines (HTB186, TE671 and D283), an erythroleukaemia cell line (HEL 92.1.7), a chronic myeloid leukaemia cell line (K-562), a follicular thyroid carcinoma cell line (RO82-W-1) and a human lung carcinoma cell line (A549). No expression was found in the human Burkitt's lymphoma cell line (Daudi). Controls lacking cDNA (shown) and controls lacking reverse transcriptase (data not shown) were negative for all samples.

SK-N-AS, which does not have amplification of *MYCN* or *MEIS1*. In contrast, the level of *MYCN* expression correlated with gene copy number in all neuroblastoma cell lines.

4. Discussion

The aim of this study was to identify sequences which are co-amplified with *MYCN* in the neuroblastoma cell line IMR-32 and to determine whether the same sequences are amplified or highly expressed in other tumour cell lines. Our CGH results confirmed previous reports of amplification of sequences from several regions of chromosome 2 in IMR-32 [20,21]. More recently, amplification of material from chromosome bands 2p13-p14 and 2p23 was found in primary neuroblastoma material suggesting that amplification in the cell line IMR-32 did not develop during *in vitro* culture [22,23].

This investigation revealed a fifth gene from the short arm of chromosome 2 which can be amplified in neuroblastoma. The *MEIS1* gene, which maps to band 2p14 [19], was found to be present in multiple copies on the HSR of IMR-32 and was also highly expressed. High levels of *MEIS1* gene expression were found in other neuroblastoma, medulloblastoma and erythroleukaemia cell lines. None of these lines had amplification of *MEIS1*, showing that the high levels of *MEIS1* expression are therefore due to alternative regulatory mechanisms. No expression of the gene was found in the Burkitt's lymphoma cell line, Daudi.

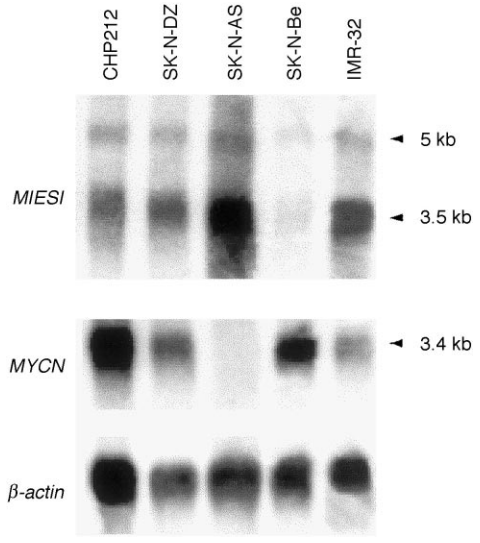

Fig. 4. Northern blot analysis of myeloid ecotropic integration site 1 (*MEIS1*) expression in the *MYCN*-amplified neuroblastoma cell lines CHP212, SK-N-DZ, SK-N-Be and IMR-32 and the neuroblastoma cell line that lacks amplification, SK-N-AS. 2 μg Poly (A)+ RNA were loaded in each lane and the blot sequentially hybridised with the *MEIS1* I.M.A.G.E. clone 223490, *MYCN* (pNb-1) and *β-actin*.

We can not exclude the possibility that the amplification of *MEIS1* in IMR-32 was accidental, and at present there is no evidence that high expression of the gene is pathogenic in human neural tissue. Nevertheless, recent findings suggest that if there is aberrant expression of the gene it might play a role in neural tumorigenesis.

MEIS1 is a member of the TALE family of homeobox genes and is thought to be important in cell proliferation [19,24]. During differentiation of bone marrow cells, expression of *MEIS1* is downregulated together with *MLL* and several *HOX* genes [25]. However, high levels of *MEIS1* expression are found in acute myeloid leukaemia cells. Association of high levels of *Meis1* gene expression and leukaemia is also seen in BXH-2 mice, where retroviral activation of *Meis1* gives rise to myeloid leukaemia [26].

The *MEIS1* protein dimerises with another TALE homeobox family member, PBX1, in normal bone marrow and in leukaemic cells [27,28]. Possible roles for *MEIS1* and *PBX1* in peripheral neural system development is suggested by analysis of *Drosophila melanogaster*. Specific binding of *homothorax*, the homologue of *MEIS1*, to *extradenticle*, the homologue of PBX1, is necessary for nuclear translocation of *extradenticle* during *Drosophila* embryonic development [29]. Correct expression of *extradenticle* is essential for embryonic growth of *Drosophila* and, of particular interest here, for correct patterning in the embryonic peripheral nervous system [30]. Aberrant expression of *MEIS1* in primitive peripheral neural tissue might thus lead to a cascade of downstream events, including aberrant nuclear localisation of PBX1, resulting in defective differentiation. One could speculate that, in combination with abnormal functioning of other genes such as *MYCN*, this process leads to neuroblastoma. Most of the neuroblastoma cell lines studied here were derived from advanced tumours. It will clearly be of interest to determine the levels of *MEIS1* expression in low-stage tumours and in normal neural tissue.

The potential significance of high expression of *MEIS1* in medulloblastoma is not clear. Medulloblastomas occur principally in the midline cerebral region, and are thought to arise from a primitive stem cell in the external granular layer of the cerebellum. Although these tumours are predominant in children, they have an older average age of onset than neuroblastoma, and are occasionally found in adults. Since *MEIS1* is expressed in all regions of the brain, and at particularly high levels in the cerebellum, further work is required to see whether the gene plays a role in medulloblastoma.

In summary, we describe co-amplification of the homeobox gene, *MEIS1*, with *MYCN* in IMR = 32 and demonstrate its high expression in other neuroblastoma cell lines. Taken together with data implicating other

homeobox genes in neuroblastoma [31], these findings warrant further investigation to determine their significance in neural differentiation and tumorigenesis.

Acknowledgements

This work was supported by the Imperial Cancer Research Fund. In addition, R.H.F and D.N. were partly supported by project grant SP2475/0101 from the Cancer Research Campaign, UK and Human Genome Mapping Project strategic grant G9422614 from the Medical Research Council, UK. We thank the HGMP resource centre for kindly providing reagents, and Jürgen Groet and Pedro Baptista for assistance with experiments.

References

1. Shimada H, Ambros IM, Dehner LP, *et al*. The International Neuroblastoma Pathology Classification (the Shimada system). *Cancer* 1999, **86**, 364–372.
2. Maris JM, Matthay KK. Molecular biology of neuroblastoma. *J Clin Oncol* 1999, **17**, 2264–2279.
3. Squire JA, Thorner PS, Weitzman S, *et al*. Co-amplification of MYCN and a DEAD box gene (DDX1) in primary neuroblastoma. *Oncogene* 1995, **10**, 1417–1422.
4. Kuroda H, White PS, Sulman EP, *et al*. Physical mapping of the DDX1 gene to 340 kb 5′ of MYCN. *Oncogene* 1996, **13**, 1561–1565.
5. Wimmer K, Zhu XX, Lamb BJ, *et al*. Co-amplification of a novel gene, NAG, with the N-myc gene in neuroblastoma. *Oncogene* 1999, **18**, 233–238.
6. Tonin PN, Yeger H, Stallings RL, Srinivasan PR, Lewis WH. Amplification of N-myc and ornithine decarboxylase genes in human neuroblastoma and hydroxyurea-resistant hamster cell lines. *Oncogene* 1989, **4**, 1117–1121.
7. Ben-Yosef T, Yanuka O, Halle D, Benvenisty N. Involvement of Myc targets in c-myc and N-myc induced human tumors. *Oncogene* 1998, **17**, 165–171.
8. Tumilowicz JJ, Nichols WW, Cholon JJ, Greene AE. Definition of a continuous human cell line derived from neuroblastoma. *Cancer Res* 1970, **30**, 2110–2118.
9. Van Roy N, Jauch A, Van Gele M, *et al*. Comparative genomic hybridization analysis of human neuroblastomas: detection of distal 1p deletions and further molecular genetic characterization of neuroblastoma cell lines. *Cancer Genet Cytogenet* 1997, **97**, 135–142.
10. Chumakov I, Rigault P, Guillou S, *et al*. Continuum of overlapping clones spanning the entire human chromosome 21q. *Nature* 1992, **359**, 380–386.
11. Ioannou PA, Amamiya CT, Kroisel PM, *et al*. A new bacteriophage P1-based vector for the propagation of large human DNA fragments. *Nature Genet* 1994, **6**, 84–89.
12. Lennon GG, Auffray C, Polymeropoulos M, Soares MB. The I.M.A.G.E. Consortium: an integrated molecular analysis of genomes and their expression. *Genomics* 1996, **33**, 151–152.
13. Senger G, Ragoussis J, Trowsdale J, Sheer D. Fine mapping of the human MHC class II region within chromosome band 6p21 and evaluation of probe ordering using interphase fluorescence in situ hybridization. *Cytogenet Cell Genet* 1993, **64**, 49–53.
14. Kallioniemi OP, Kallioniemi A, Piper J, *et al*. Optimizing comparative genomic hybridization for analysis of DNA sequence copy number changes in solid tumors. *Genes Chrom Cancer* 1994, **10**, 231–243.
15. Telenius H, Carter NP, Bebb CE, Nordenskjold M, Ponder BA, Tunnacliffe A. Degenerate oligonucleotide-primed PCR: general amplification of target DNA by a single degenerate primer. *Genomics* 1992, **13**, 718–725.
16. Bentley DR, Todd C, Collins J, *et al*. The development and application of automated gridding for efficient screening of yeast and bacterial ordered libraries. *Genomics* 1992, **12**, 534–541.
17. Sambrooke J, Fritsch EF, Maniatis T. *Molecular Cloning: a Laboratory Manual*. Cold Spring Harbour, New York, Cold Spring Harbour Laboratories, 1989.
18. Groet J, Ives JH, South AP, *et al*. Bacterial contig map of the 21q11 region associated with Alzheimer's disease and abnormal myelopoiesis in Down syndrome. *Genome Res* 1998, **8**, 385–398.
19. Smith JE Jr, Bollekens JA, Inghirami G, Takeshita K. Cloning and mapping of the MEIS1 gene, the human homolog of a murine leukemogenic gene. *Genomics* 1997, **43**, 99–103.
20. Shiloh Y, Shipley J, Brodeur GM, *et al*. Differential amplification, assembly, and relocation of multiple DNA sequences in human neuroblastomas and neuroblastoma cell lines. *Proc Natl Acad Sci USA* 1985, **82**, 3761–3765.
21. Zitzelsberger H, Lehmann L, Werner M, Bauchinger M. Comparative genomic hybridisation for the analysis of chromosomal imbalances in solid tumours and haematological malignancies. *Histochem Cell Biol* 1997, **108**, 403–417.
22. Brinkschmidt C, Christiansen H, Terpe HJ, *et al*. Comparative genomic hybridization (CGH) analysis of neuroblastomas — an important methodological approach in paediatric tumour pathology. *J Pathol* 1997, **181**, 394–400.
23. Lastowska M, Nacheva E, McGuckin A, *et al*. Comparative genomic hybridization study of primary neuroblastoma tumors. United Kingdom Children's Cancer Study Group. *Genes Chrom Cancer* 1997, **18**, 162–169.
24. Steelman S, Moskow JJ, Muzynski K, *et al*. Identification of a conserved family of Meis1-related homeobox genes. *Genome Res* 1997, **7**, 142–156.
25. Kawagoe H, Humphries RK, Blair A, Sutherland HJ, Hogge DE. Expression of HOX genes, HOX cofactors, and MLL in phenotypically and functionally defined subpopulations of leukemic and normal human hematopoietic cells. *Leukemia* 1999, **13**, 687–698.
26. Moskow JJ, Bullrich F, Huebner K, Daar IO, Buchberg AM. Meis1, a PBX1-related homeobox gene involved in myeloid leukemia in BXH-2 mice. *Mol Cell Biol* 1995, **15**, 5434–5443.
27. Knoepfler PS, Calvo KR, Chen H, Antonarakis SE, Kamps MP. Meis1 and pKnox1 bind DNA cooperatively with Pbx1 utilizing an interaction surface disrupted in oncoprotein E2a-Pbx1. *Proc Natl Acad Sci USA* 1997, **94**, 14553–14558.
28. Shen WF, Rozenfeld S, Kwong A, Komuves LG, Lawrence HJ, Largman C. HOXA9 forms triple complexes with PBX2 and MEIS1 in myeloid cells. *Mol Cell Biol* 1999, **19**, 3051–3061.
29. Rieckhof GE, Casares F, Ryoo HD, Abu-Shaar M, Mann RS. Nuclear translocation of extradenticle requires homothorax, which encodes an extradenticle-related homeodomain protein. *Cell* 1997, **91**, 171–183.
30. Kurant E, Pai CY, Sharf R, Halachmi N, Sun YH, Salzberg A. Dorsotonals/homothorax, the Drosophila homologue of meis1, interacts with extradenticle in patterning of the embryonic PNS. *Development* 1998, **125**, 1037–1048.
31. Smith MD, Latchman DS. The functionally antagonistic POU family transcription factors Brn-3a and Brn-3b show opposite changes in expression during the growth arrest and differentiation of human neuroblastoma cells. *Int J Cancer* 1996, **67**, 653–660.